PREPARATION OF A GOLD NANOPARTICLE CONTAINING ELECTROSPUN POLY (Ɛ -CAPROLACTONE) SCAFFOLD FOR STEM CELL DIFFERENTIATION

by

Hamide Özaydın

Submitted to Graduate School of Natural and Applied Sciences
in Partial Fulfillment of the Requirements
for the Degree of Master of Science in
Biotechnology

Yeditepe University
2015

PREPARATION OF A GOLD NANOPARTICLE CONTAINING ELECTROSPUN POLY (Ɛ-CAPROLACTONE) SCAFFOLD FOR STEM CELL DIFFERENTIATION

APPROVED BY:

Prof. Dr. Mustafa Çulha
(Thesis Supervisor) .....

Assoc. Prof. Bahattin Koç .....

Asst. Prof. Andrew J. Harvey .....

DATE OF APPROVAL: .../.../2015

ACKNOWLEDGEMENTS

It is with immense gratitude that I acknowledge the support and help of my Professor Mustafa Çulha. Pursuing my thesis under his supervision has been an experience, which broadens the mind and presents an unlimited source of learning.

I also thank Professor Fikrettin Şahin, Professor Cem Ünsalan, and Research Assistants; Manolya Kukut, Ertuğ Avcı, Gamze Kuku, Mine Altunbek, Seda Keleştemur, Hande Duru and Zehra Çobandede.

Finally, I would like to thank my family and my colleague for their endless love and support, which makes everything more beautiful.

ABSTRACT

PREPARATION OF A GOLD NANOPARTICLE CONTAINING ELECTROSPUN POLY (Ɛ -CAPROLACTONE) SCAFFOLD FOR STEM CELL DIFFERENTIATION

Nerve tissue engineering aims to improve the nerve repair and regeneration rate. Electrical stimulation has an influence on the adipose stem cell differentiation into neuronal cells. The developed hypothesis argues that gold nanoparticle (AuNP) incorporated Poly (ε -caprolactone) (PCL) scaffolds can be applied in nerve tissue engineering. Although PCL is a non-conductive and highly hydrophobic polymer, it is commonly used for nerve tissue engineering. The hydrophilicity, which is necessary for cell attachment and proliferation is provided by AuNPs. Also, AuNPs give electrical conductivity to non-conductive PCL polymer. In this study, an AuNP containing extracellular matrix for differentiation of human adipose stem cells was developed by preparing a scaffold using electrospinning technique. In order to provide conductivity, the aqueous alkaline sodium borohydride reduced AuNPs were blended into the PCL. The AuNP containing PCL scaffold was composed of fibers in the size range of 3 to 6 μm. The aim was to easily differentiate human adipose stem cells (HASCs) into neuronal cells using electrical stimulation throughout AuNPs. This study is promising a new regeneration method for the neuronal cell differentiation.

ÖZET

KÖK HÜCRE FARKLILAŞMASI IÇIN ALTIN NANOPARCACIK İÇEREN ELECTROSPUN POLY (Ɛ -CAPROLACTONE) SCAFFOLD HAZIRLANIŞI

Sinir hücresi doku mühendisliğinin amacı sinir hücresi yenilenmesi ve onarımının düzeyini arttırmaktır. Elektriksel uyarım yağ dokusundan elde edilen kök hücrelerin sinir hücresine dönüşmesi için kullanılabilen bir araçtır. PCL içine konulmuş AuNP'ler hücre dışı matriksi sinir doku mühendisliğinin başarılabilir olduğunu önesürmektedir. Poly (ε -caprolactone) (PCL) yalıtkan ve oldukça hidrofobik bir polimer olmasına rağmen sinir doku mühendisliğinde yaygın olarak kullanılır. Hücre tutunması ve hücre çoğalması için gerekli olan hidrofilikliği AuNP'ler tarafından sağlanmaktadır. AuNP'ler yalıtkan PCL polimerine iletkenlik kazandırır. Bu çalışmada insan yağ dokusundan izole edilen kök hücreler için yapay hücre dışı matriksi, electrospinning tekniği kullanılarak hazırlanmıştır. Elektriksel iletimi sağlamak üzere alkaline sodium borohydride tarafından indirgenmiş AuNP'ler, PCL polimeri ile karıştırılmıştır. PCL/AuNP yapay hücre dışı matriksinin fiber çapı 3 ile 6 μm arasındadır. AuNP'ler aracılığıyla elektriksel uyarım kullanılarak yağ dokudan izole edilen kök hücrelerin kolaylıkla sinir hücrelerine dönüşmesi beklenmektedir. Bu çalışma gelecekte sinir hücrelerinin farklılaşması için yeni bir metod vaad etmektedir.

TABLE OF CONTENTS

LIST OF FIGURES

LIST OF TABLES

LIST OF SYMBOLS/ABBREVIATIONS

AFM	atomic force microscopy
AuNPs	gold nanoparticles
DCM	dichloromethane
DLS	dynamic light scattering
ECM	extra cellular matrix
HASCs	human adipose stem cells
MSCs	mesenchymal stem cells
PCL	poly (ε -caprolactone)
PEG	poly (ethylene glycol)
PEO	poly (ethylene oxide)
PLGA	poly (D,L-lactic–co–glycolic acid)
PLLA	poly(L-lactic acid)

1. INTRODUCTION

As defined by Langer and Vacanti, tissue engineering is a multidisciplinary field combining engineering and life sciences. It enables production of functional tissue replacements and organs *de novo* as well as development of biological substitutes for tissue regeneration [1].

Tissue engineering provides two approaches for tissue regeneration and repair, through non-cellular or cellular techniques [1-2]. The former includes the use of tissue from the host organ, which is incorporated on a non-cellular matrix called as tissue engineering scaffold. In the second method, donor cells are directly injected into the host or seeded on scaffolds before implantation.

Tissue engineering works on scaffolds, cells, and mechanical or biochemical stimuli. Their ability to self-renewal and to differentiate into many cell types makes stem cells a promising choice for tissue engineering applications.

The stem cells are classified into two groups; human embryogenic stem cells and adult stem cells. Human embryogenic stem cells are isolated from the inner cell mass of embryo, which is at the undifferentiated state and have limitless supply of pluripotent cells [2]. The adult stem cells are discovered from the adult bone marrow, which was pertaining blood, known as hematopoietic stem cells. Bone marrow or subcutaneous adipose tissues provide pluripotent progenitor stem cells known as mesenchymal stem cells (MSCs). This type of MSCs gives same differentiation potential into cells and tissues of mesodermal origin, which are cartilage, bone and skeletal muscle, adipocytes [3]. Human adipose tissue is an essential source to help tissue regeneration by adipose-derived stem cells (ASCs), which are also examined in the laboratory for a wide range of cell-based therapies [4-5]. The adipose tissue-derived mesenchymal cells (ATMSCs) provide some advantages with the ease of access to subcutaneous adipose tissue and simple isolation procedures in regenerative tissue engineering. The bone marrow-derived MSCs and human ASCs are very similar in morphology and phenotype. However, there are some differences between them. For instance, adipose tissue collection is less traumatic than bone marrow harvest, and the frequency of stem cells is higher in that tissue. Thus, ASCs demonstrate an attractive and efficient cell type for regenerative medicine [5].

ASCs provide some properties to be extensively preferred for tissue engineering applications such as ease of availability and ease of retrieval. However, if the phonotype expression and differentiated functions of stem cells are to be maintained, a simulated microenvironment has to be generated. The three dimensional (3D) environment is required if the full potential of stem cells is to be uncovered. 3D micro-environment (scaffold) correlates with their renewal, differentiation and assembly in the native tissue [6-7].

1.1. SCAFFOLD PREPARATION

Human body organizes the cell and tissue behavior, and tissue engineering contributes to this organization by providing improvement and design of synthetic extracellular matrix (ECM) similar to novel biomaterials, which encourages 3D cell culture and tissue regeneration [8]. Scaffolds provide not only mechanical support to the cell attachment but also proliferation, differentiation, apoptosis and migration by influencing cells with biochemical signals and topological cues [9]. The scaffold materials can be successfully made up in tissue engineering, it is necessary to interact between the cells and the environment.

The conventional scaffold fabrication techniques can produce scaffolds smaller than 10 μm in diameter, which can mimic ECM by giving as much as geometrical and architectural properties for the cell attachment and proliferation. The three production methods commonly used in tissue engineering are phase separation, self-assembly and electrospinning technique [10]. Each technique includes its own set of advantages and disadvantages. Tissue engineering scaffolds can be prepared using a range of methods. The most important ones are summarized below.

1.1.1. Phase Separation Method

The porous polymer has been created by phase separation method, which includes two different phases as low polymer phase and a high polymer phase. The phase separation method is important because it provides tunable phase separation synthesis of the polymer

solution. After phase separation, the phase compact is concentrated and it shapes the membrane that is to simultaneously become solid (Figure 1.1.) [11].

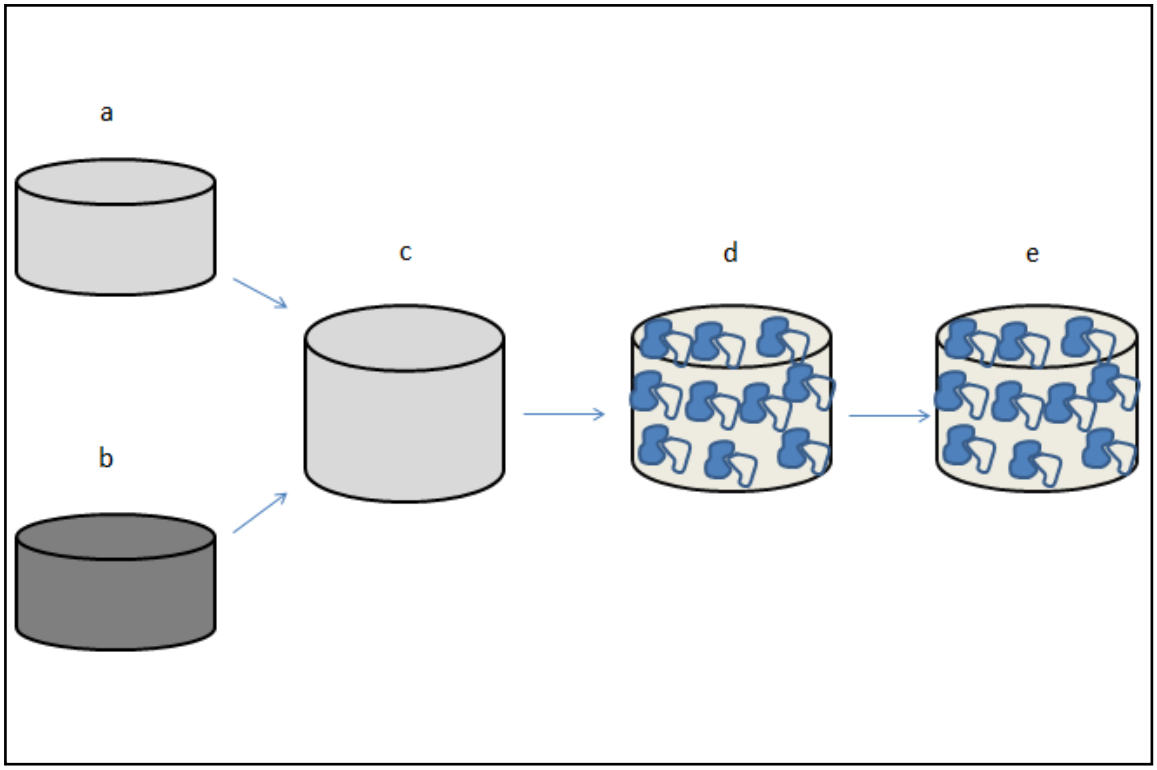

Figure 1.1. Polymer (a) and solvent (b) are mixed (c). This mixed solution is quickly frozen which causes phase separation (d) of the polymer and solvent. After all, the solvent is eliminated (e).

The scaffold generally has been used to produce from aliphatic polyesters such as PLLA [12] and PLGA [13]. There are variety of factors which affect phase separation such as gelling temperature which is important for phase separation method generally use to acquire of nanofiber. Microfiber scaffolds can prepare with high gelling temperature and low gelling temperature provides to reduce to fiber formation [14]. Besides, polymer concentration does not influence of the fiber diameter. This method does not require special equipment and it can be shaped in many possible geometries. However, this method uses toxic solvents [14].

1.1.2. Self-assembly Method

Self-assembly method correlates noncovalent interactions such as hydrogen bonds, Van der Waals, electrostatic and hydrophobic interactions between small molecules, peptides, proteins and nucleic acids [15]. The aims of self-assembly method are to incorporate particular biological components of the ECM and also imitate the assembly of the ECM using bottom-up strategy [16]. The commonly used molecule is peptide amphiphile (PA) in this method. PA includes long alkyl tail, which contributes to the hydrophobic characteristics to use the self-assembly. PA has also cysteine residues to create disulfide bonds for polymerization. Furthermore, the three glycine residues are used in the linker region, which provides flexibility to the hydrophilic head group (Figure 1.2.) [17-18]. In this manner, the peptides used for the hydrophilic head groups mimic ECM for improving cell attachment.

However, the most important criteria for cell attachment are the pore size and pore structures. The self-assembly method is easy to apply but it is limited in its ability to form macro-pores, which are main properties for cell migration and proliferation. Another drawback is biocompatibility because many enzymes can easily degrade the peptide backbone [19].

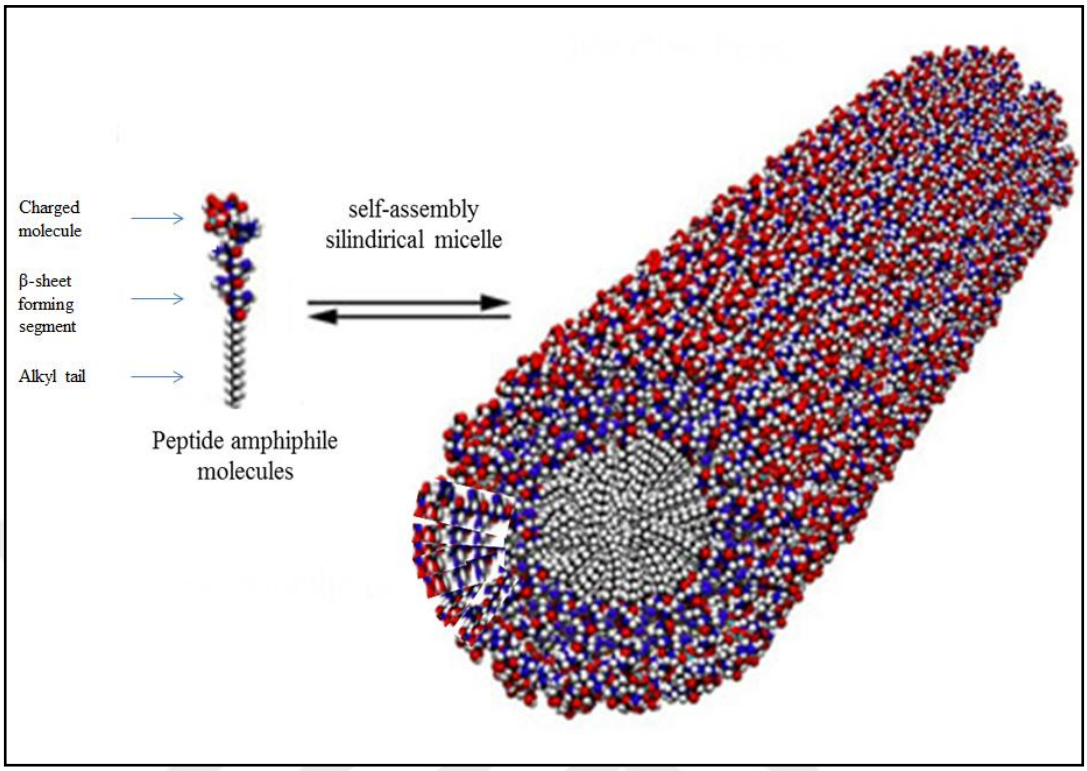

Figure 1.2. **S**elf-assembled morphology of peptide amphiphiles, which are common building blocks for self-assembly method. Figure modified from ref.[39].

1.1.3. Electrospinning Method

Due to its simplicity and low cost, electrospinning technique is the most common method to produce fiber meshes in tissue engineering. This technique facilitates production of long and continuous fibers ranging from 5 nm to 12 μm in diameter [20]. The electrospinning process occurs when electrostatic repulsion at the polymer solution surface to overcome the surface tension. Then, it causes electrically charged jet to be ejected. The polymer solution evaporates from the needle and the metallic collector collects the charged polymer fibers randomly, as shown in Figure 1.3.

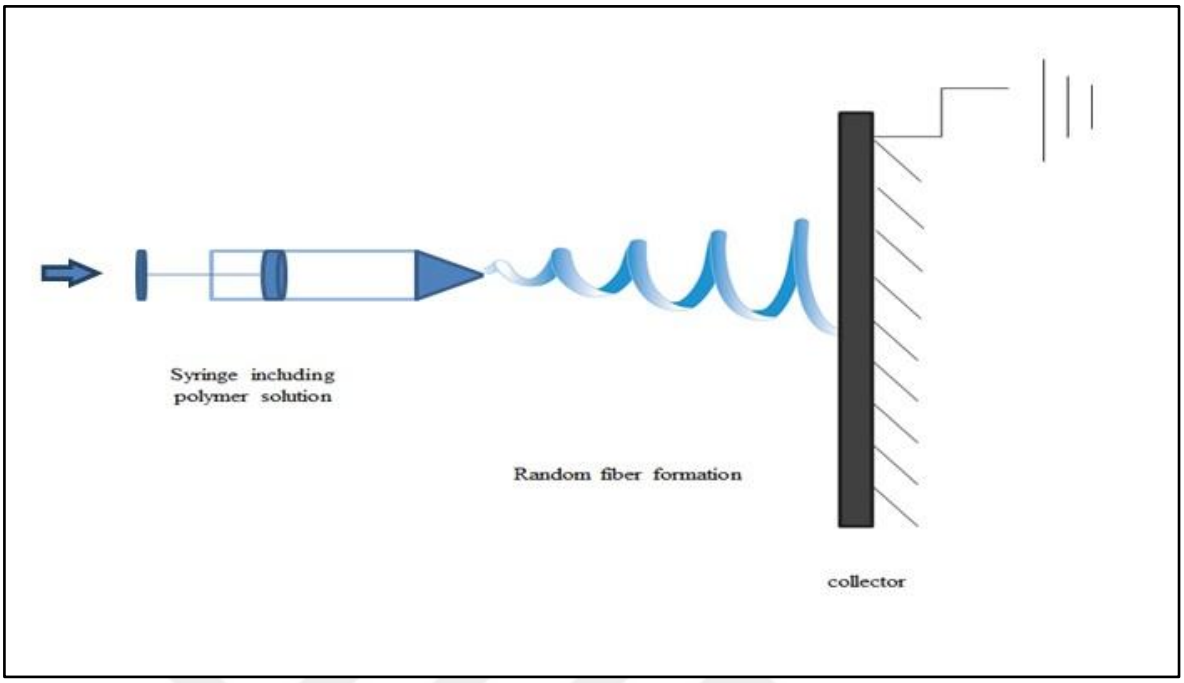

Figure 1.3**.** Electrospinning setup containing three parts; the first is a syringe pump containing the polymeric materials; the second part is a high voltage source to generate high electric field for spinning and third part is a metallic collector collecting the fibers.

It is possible to make some adjustments in this method to control the fiber diameter such as concentration of polymer dissolved in solution, magnitude of applied voltage and distance from needle to the collector [20-18]. The advantage of electrospinning method is to have a simple and effective procedure. Also, the electrospinning set-up is inexpensive. Furthermore, the fiber diameter, orientation and viscosity can be controlled easily.

There are some natural and synthetic polymers to be used in electrospinning method. Generally, synthetic polymers are much easier to apply than natural polymers for electrospinning applications [21]. Natural polymers are generally blended with synthetic polymers in this way. Solution viscosity and solution consistency can also be increased in electrospinning. For example, poly (ethylene oxide) (PEO) is blended with chitosan, which causes to increase the chain entanglements. At the same time this mixture causes to decrease the conductivity of charged polysaccharide solution [22]. Other natural polymers, gelatin and collagen, can be used to decrease the electrospun fiber diameter as small as 100 nm and also mimic native collagen. Synthetic polymers include poly (lactic) acid (PLA) [23], poly (ethylene glycol) (PEG) [23], and poly (ε -caprolactone) (PCL) [24]. The

synthetic polymer PCL has been utilized due to its favorable mechanical strength and biodegradable properties for the tissue engineering.

The endogenous electrical stimulation is a crucial cue for many biological processes such as maintaining cellular homeostasis, embryonic growth, wound healing [25-26]. The morphogenesis is triggered without the electrical stimulation on biological processes. The electrical stimulation is used to establish, to regenerate and to recover the lost function, after spinal cord injury [27]. In this case, several *in vitro* experiments have demonstrated the role of exogenous electrical stimulation on regulation mechanism such as transmembrane channel activation, change in intracellular calcium ion level and cell surface receptor accumulation [28-29].

The electrical stimulation is important for the tissue development such as wound healing and signaling of the nervous system. The electrical field of the major cellular activities such as cell division and migration was reported by McCaig *et al.* [30]. Another study also reported weak direct current (DC) affects cell migration and differentiation. The exogenous electrical stimulation correlated with direct nerve cell growth [31]. The typical membrane potential is 100 mV and the observation of stem cell differentiation, which were treated with electrical stimulation, caused to the assumption of neuronal fate from stem cells [32]

The electrical stimulation also plays an important role on stem cell response. MAPK, PI3K and ROCK signalling pathways are activated with electrical stimulation on multipotent adipose derived stromal cells [33]. In another study, MSCs migrated to injured sites under electrical stimulation, which leaded to wound healing [34]. Furthermore, Gardner *et al*. demonstrated that the chronic wound healing is increased by electrical stimulation [35]. Perry *et al*. showed that significant treatment of skin scar is influenced by the biofeedback electrical stimulation [36]. Another study is that after bone marrow-derived mesenchymal stromal cells (BMMSCs) transplantation, the electrical stimulation improved the treatment of spinal cord injury and also the functional recovery was enhanced [27]. Patient age and the number of problematic scars present affect response to biofeedback electrical stimulation. Further controlled studies are necessary. The current studies has shown that management of symptomatic abnormal skin scarring is posibble by the use of biofeedback electrical stimulation.

New developments in the field of scaffold engineering provide the design of biomimetic scaffolds, both blended with signaling biomolecules or surface attachment. The controlled delivery of biochemical signals such as cytokines, growth factors or other environmental cues causes the cells to attach on the scaffold and it gives proliferation, differentiation, and secretion of the ECM components required to create the desired new tissue. Furthermore, the mechanical signal such as electrical stimulation provides same features to the cells. In this study the idea is to prepare biomimetic PCL/AuNPs scaffolds to support cell attachment and proliferation.

2. MATERIAL AND METHODS

2.1. COLLOIDAL GOLD NANOPARTICLE PREPARATION

Aqueous phase AuNPs were prepared with sodium borohydride ($NaBH_4$) (MERCK, 845048). Chloroauric acid (Sigma, 520918-5G)was prepared by dissolving 180 mg chloroauric acid in 10 ml of water to make it 50 mM. A 50 mM alkaline sodium borohydride solution was also prepared by dissolving equimolar quantities of $NaBH_4$ and NaOH in water. A 50 mM chloroauric acid solution was added into 97 ml distilled water, and then 2.7 ml of 50 mM prepared alkaline $NaBH_4$ solution was added into it.

The synthesized AuNPs were phase transferred from water to hexane using a version of Martin's protocol [37]**.** A 75 ml of acetone was added into a 100 ml of AuNP suspension and the mixture was shaken about 30 s. A 25 ml of hexane, which includes 1 µl 4.57 M 1-undecanethiol, was placed into the mixture. This suspension was shaken 15 min by hand, and then incubated at room temperature for 15 min. The suspension waited to separate into two phases. In the top phase, the color was redish, which included hexane phase with AuNPs. A 5 ml of toluene was added into the hexane including AuNPs, and then the suspension was heated until hexane was evaporated.

A 16 % (w/v) of PCL was prepared with 1:1 dichloromethane (DCM):Toluene/AuNPs, which was incubated overnight on shaker. Following this procedure, the DCM and toluene was evaporated. After that, the PCL/AuNPs was mixed with DCM.

2.2. CHARACTERIZATION OF COLLOIDAL GOLD NANOPARTICLES

The colloidal gold nanoparticle size and size distribution were analyzed by dynamic light scattering (DLS) (Nanozetasizer, Malvern) at 25^{o}C. Distilled water and toluene were used as diluting medium for AuNPs.

UV visible spectrophotometer (Lambda 25, Perkin Elmer) was used to obtain the dispersion difference between AuNPs in double distilled water (ddH_2O) and AuNPs in toluene.

The AFM analysis of AuNPs was carried out Atomic force microscopy (AFM) (Park Systems XE 100). The silicon nitride tip was used at room temperature. A 3 μL of AuNPs suspension was put onto the glass surface and waited to dry for 30 min. The AFM images were analysed by using XEI, an image-processing program for SPM data developed by PSIA.

2.3. ELECTROSPINNING

16 % (w/v) PCL/AuNPs and %16 PCL, which was prepared by electrospinning technique was mixed in DCM and incubated overnight while stirring. The polymer solution was placed into a 5 ml glass syringe fitted with a needle with a tip diameter of 0.4 mm. The PCL/AuNPs solution and PCL solution was fed to the needle tip using a syringe pump at a flow rate 1 $ml.h^{-1}$. A high positive voltage of 10 kV was applied to the needle connected to the syringe when the solution came out of the syringe.

2.4. CELL CULTURE EXPERIMENTS AND CELL MORPHOLOGYCAL OBSERVATION

The HASCs isolated from human adipose tissue and growth in medium containing DMEM (Dulbecco's modified eagle's medium - low glucose; Sigma) supplemented with 10% FBS (Fetal bovine serum; Sigma), % 1 antibiotic solution (Sigma). The cells were grown in 5% CO_2 incubator at 37^oC (Auto Flow CO_2 incubator 8500, Nuaire). 0.05% trypsin-EDTA (Sigma, Germany) was used to move cells, which were completed with complete media and centrifugation at 1100 rpm for 5 min.

The morphology of HASCs grown on PCL and AuNPs/PCL micro-fibrous scaffolds were examined after 7 days of culture in the medium including 10% FBS and 1% PSA in the presence of electrical stimulation of 10 minutes a day (min/day). The PCL and PCL/AuNPs scaffolds were cut into squares of 1 cm x 1 cm dimensions. The scaffolds

were sterilized with 70% ethanol for 24 h, followed by washing with PBS 3 times for 5 min before cell seeding. A seeding density of 5 x 10^5 cells/ml was used for this study.

After 7 days of culture with electrical stimulation, the micro-fibrous including the cells scaffolds were washed three times with PBS and were fixed with 2.5% glutaraldehyde for 30 min. Afterwards, scaffolds were washed with PBS 3 times for 5 min.

The morphology of the microfiber scaffolds were characterized by scanning electron microscope (SEM) (Carl Zeis Evo-40) after gold coating (Baltec SDC 005 sputter-coater) at an accelerating voltage of 25 kV. Diameters of the microfiber scaffolds were analyzed from the SEM images using image analysis software.

2.5. ELECTRIC FIELD SET UP

Direct current (DC) (Hp 3620 A) electrical field were used in this experiment. The electrical stimulation was provided by two stainless steel probes and kept on two ends of sterile tissue culture. The 1 cmx 1 cm PCL and PCL/AuNPs micro-fibrous scaffolds were positioned at the centre between steel and the direction of the applied electric field was parallel to the scaffold surface. DC source was examined 100 mV.

All HASCs culture samples were incubated 3 days on the PCL and PCL/AuNPs micro-fibrous scaffolds and then DC electric field was applied for 10 min a day for 5 days both on PCL and AuNPs micro-fibrous scaffolds including HASCs.

2.6. WST-1 ASSAY

WST-1 cell viability assay was used (Roche Diagnostics, Roche) on the cells seeded on PCL and PCL/AuNPs scaffolds. The HASCs of approximately 5 x 10^5cells/ml were seeded on the sterilized scaffolds placed in 96-well plates and were grown in a CO_2 incubator at 37^{o}C. After culturing the cells for a period of 7 days, the medium in the well plate was removed and washed twice with PBS. WST-1 reagent was prepared in DMEM and incubated for 1 h at 37^{o}C. The absorbance of the obtained dye was at 420 nm using a spectrophotometric plate reader (ELx800 Absorbance Reader, Bio-Tek Instruments). The readings were taken after 7 days. The WST-1 assay was performed in triplicates.

2.7. FLOW CYTOMETRIC ANALYSIS

The HASCs were grown on PCL and PCL/AuNPs microfibrous scaffolds and were stimulated with electrical field of 100 mV/cm in cycles of 10 min/day for 5 days. After the incubation, the HASCs were trypsinized, centrifuged and the trypsin was moved from cells. 2% paraformaldehyde was used for fixation and incubated at +4 ˚C for half an hour. Fixed HASCs were centrifuged. The pellets were treated with two different primary antibodies, which were MAP2 and Nestin, overnight at +4˚C. 1 ml PBS was added into the primary antibody and centrifuged. The pellet was dissolved in secondary antibody for MAP2 to Alexa flour 647 and Nestin to Alexa flour 488 for 1 hour. Following this, the HASCs were washed with PBS and centrifuged at 2500 rpm for 5 min. At the end, HASCs were resuspended in 500 µl PBS and analyzed using Guava easyCyte flow cytometer (Merck-Millipore).

2.8. WETTABILITY

Hydrophilicity/hydrophobicity of the PCL microfibrous scaffolds before and after AuNP scaffolds were determined by sessile drop water contact angle measuring system (KSV, CAM 100) with a charged coupled device (CCD) camera. The droplet size was set at 0.5 µl. Distilled water was used for drop formation. The measurements were done in triplicates for PCL and PCL/AuNPs micro-fibrous scaffolds.

2.9. IMMUNOCYTOCHEMISTRY

HASCs were grown on PCL and PCL/AuNPs micro-fibrous scaffolds for 5 days, which were processed for immunocytochemistry experiments to detect expression of β-III Tubulin and Nestin. The HASCs were fixed with 2% paraformaldehyde at room tempreture for 30 min. The cells were incubated with primary antibodies, anti-Nestin antibody (1/200, Abcam) and anti-β-III Tubulin (1/200, Abcam), overnight at $+4^0$C. The secondary antibody, Alexa Flour 488 conjugated goat anti-mouse IgG (1/500, Abcam), was incubated for 1 h at room temperature. The cells were washed with PBS and nuclear stain Hoechst 33258 (1ug/ml in PBS) was added for 5 min. The washing procedure was carried

out 3 times with PBS before mounting on to glass slide and the samples were examined under confocal microscope (Zeiss LSM 700).

3. RESULTS

3.1. MORPHOLOGY, CHEMICAL AND MECHANICAL CHARACTERIZATION OF MICROFIBERS SCAFFOLDS

Figure 3.1. shows the DLS results of AuNPs in dH_2O and in toluene. The hydrodynamic size of the AuNPs in dH_2O and the AuNPs in toluene were at 5.6 ± 2 nm and 4.8 ± 2 nm, respectively.

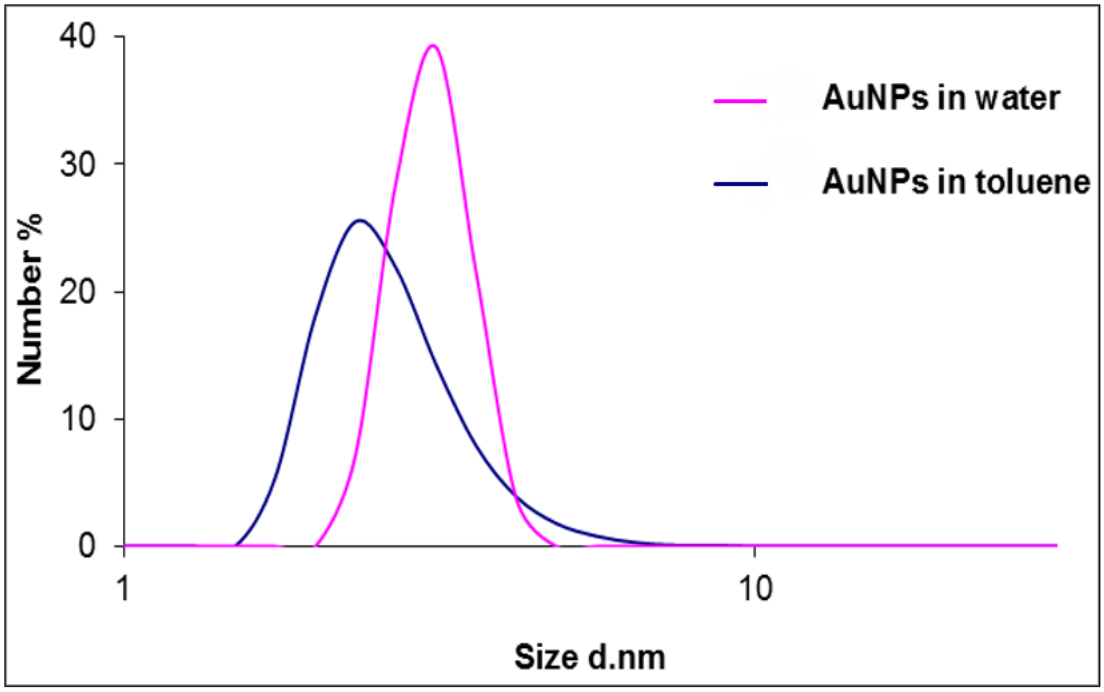

Figure 3.1. Size of AuNPs in water and toluene

The UV-visible spectra of the AuNPs dispersed in dH_2O and in toluene are showon on Figure 3.2.

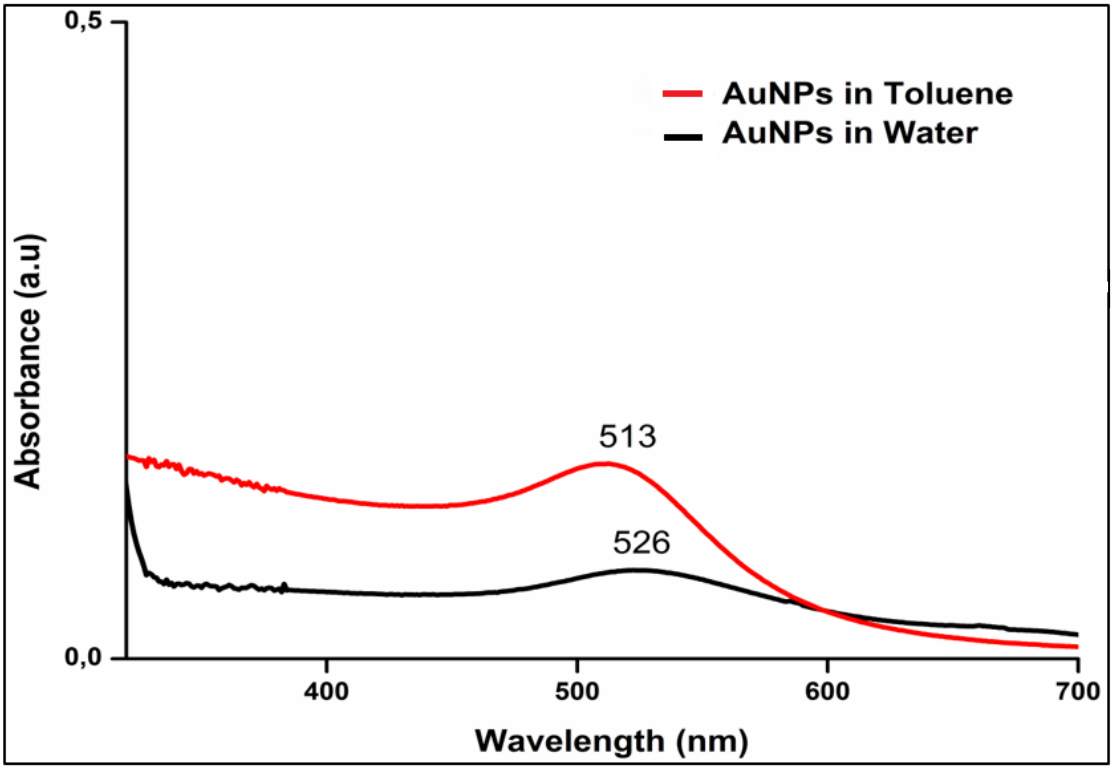

Figure 3.2. UV/Vis spectra of AuNPs in toluene (black) and in water (red).

The AFM images of the AuNPs on a glass surface is provided on Figure 3.3.

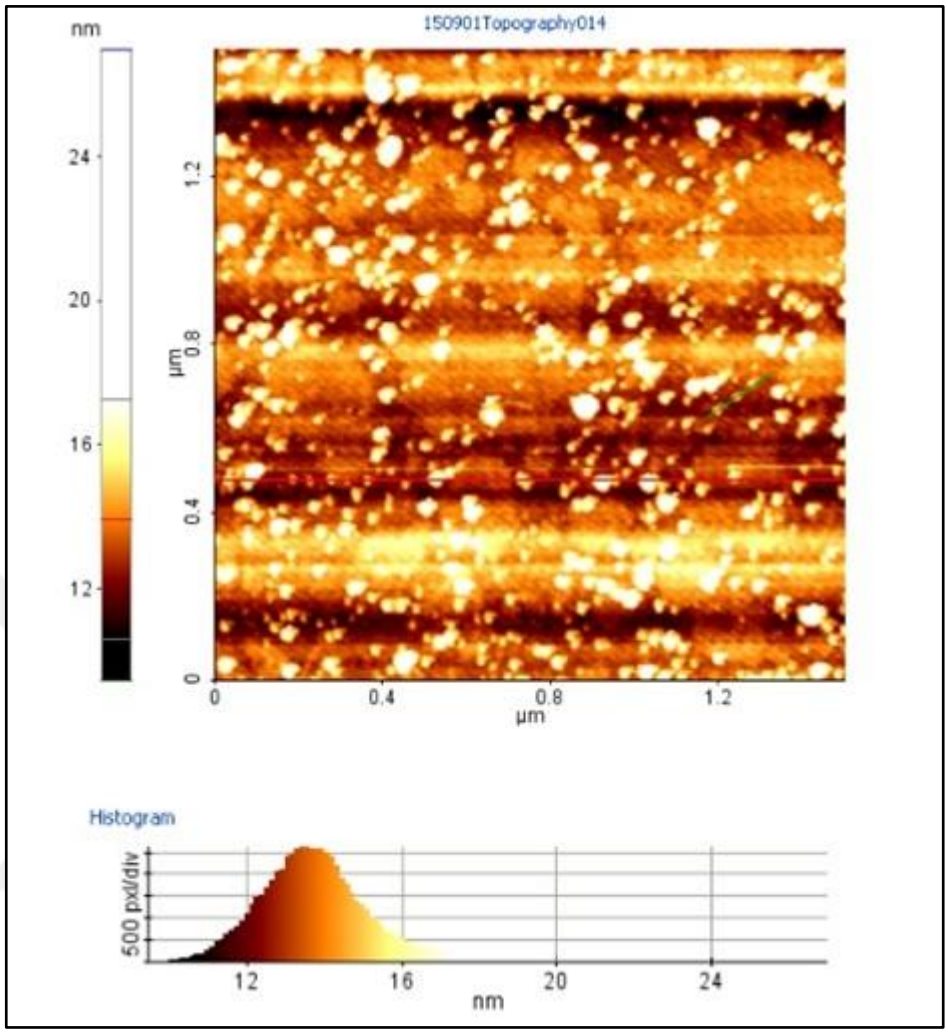

Figure 3.3. Representative AFM image of AuNPs on glass surface.

The PCL micro-fibrous were determined to be substantially hydrophobic and the contact angle measurements were 133 ± 5^{o}. Nevertheless, the contact angles with PCL/AuNPs scaffolds were determined more hydrophilic than PCL scaffolds as also shown in Table 3.1. Figure 3.4.

Table 3.1. Contact angle measurement of PCL and PCL/AuNPs micro-fibrous scaffolds

Substrate	**Contact Angle (^{o})**
PCL	133 ± 5
PCL/AuNPs	127 ± 3

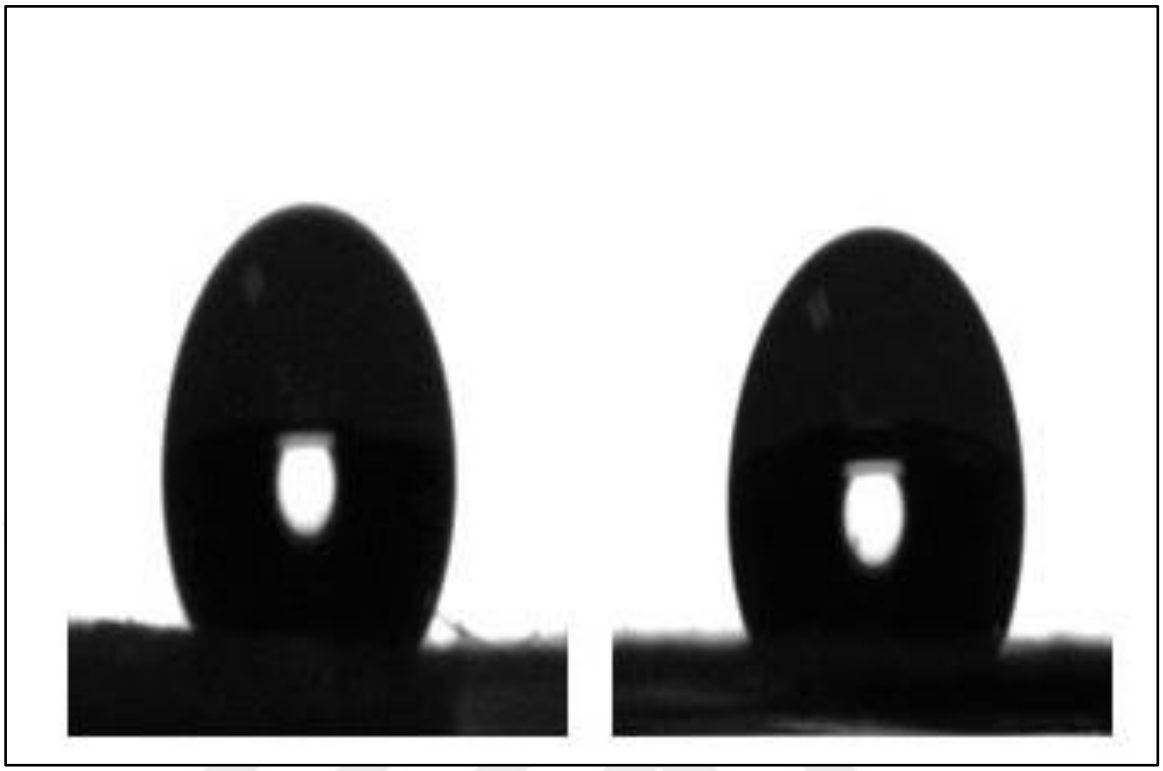

Figure 3.4. Water contact angle of PCL (left) and AuNPs/PCL (right) micro-fibrous scaffolds.

The SEM images of micro-fibrous scaffold structures show that they consist of random fiber structures under the optimized spinning conditions evaluated during this study as seen in Figure 3.5.-3.6. Uniform random microfibers of PCL and PCL/AuNPs were observed with the fiber diameter in the range of 3 to 5 μm and 3 to 6 μm, respectively.

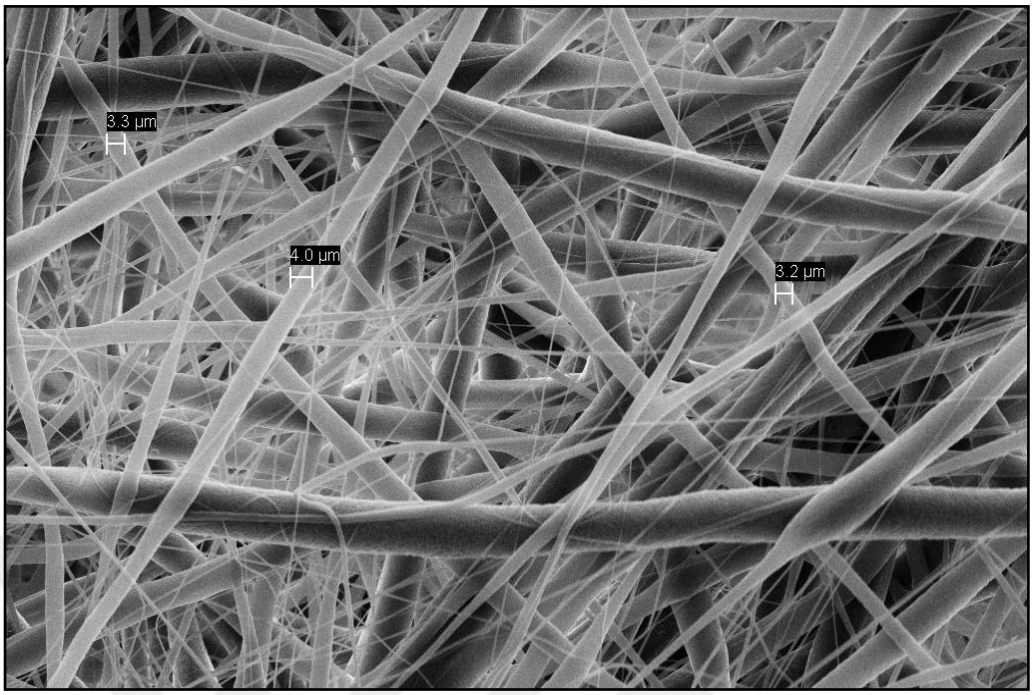

Figure 3.5. SEM image of 16% PCL. Average size of PCL scaffolds are 4 µm.

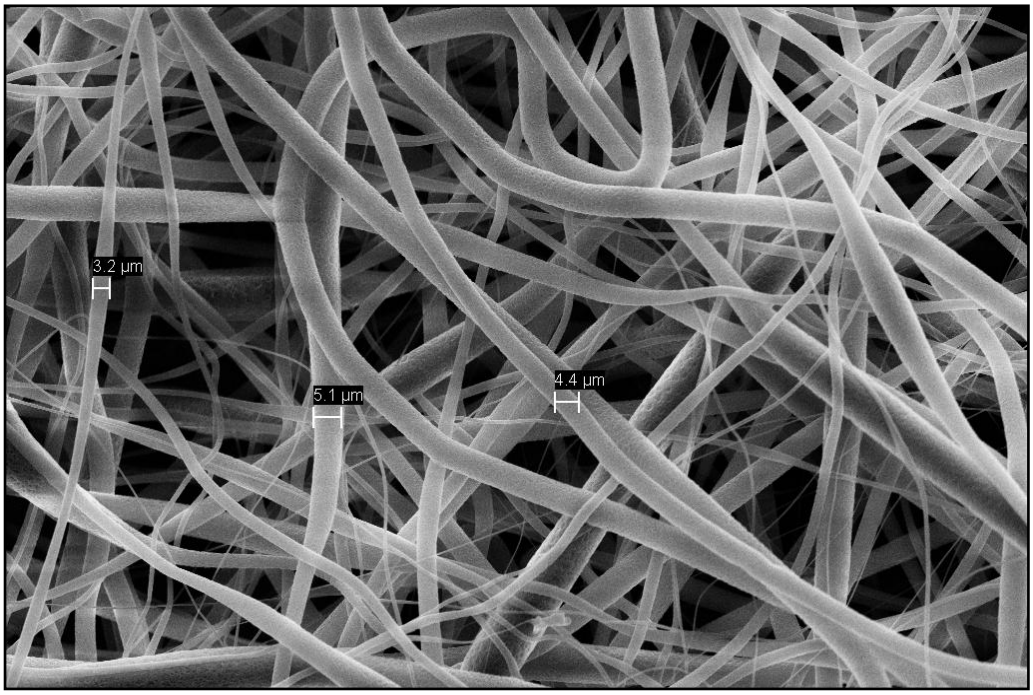

Figure 3.6. SEM image of 16% PCL/AuNPs. The average sizes of PCL/AuNPs scaffolds are 5 +/-stdv µm.

3.2. CELL SCAFFOLD INTERACTION

In vitro studies were carried out using HASCs .SEM images exhibited the cells interaction on PCL and PCL/AuNPs micro-fibrous scaffolds for first day in Figure 3.7.-3.8., respectively. Figure 3.10. and 3.12. showed that the AuNPs incorporated into PCL scaffolds was found to promote HASCs interaction more than PCL micro-fibrous scaffolds and cells with less interaction after 3^{th} and 7^{th} day as seen on Figure 3.9.-3.11.

Figure 3.7**.** The 1^{st} day of proliferation HASCs on PCL.

Figure 3.8. The 1st day of proliferation HASCs on PCL/AuNPs.

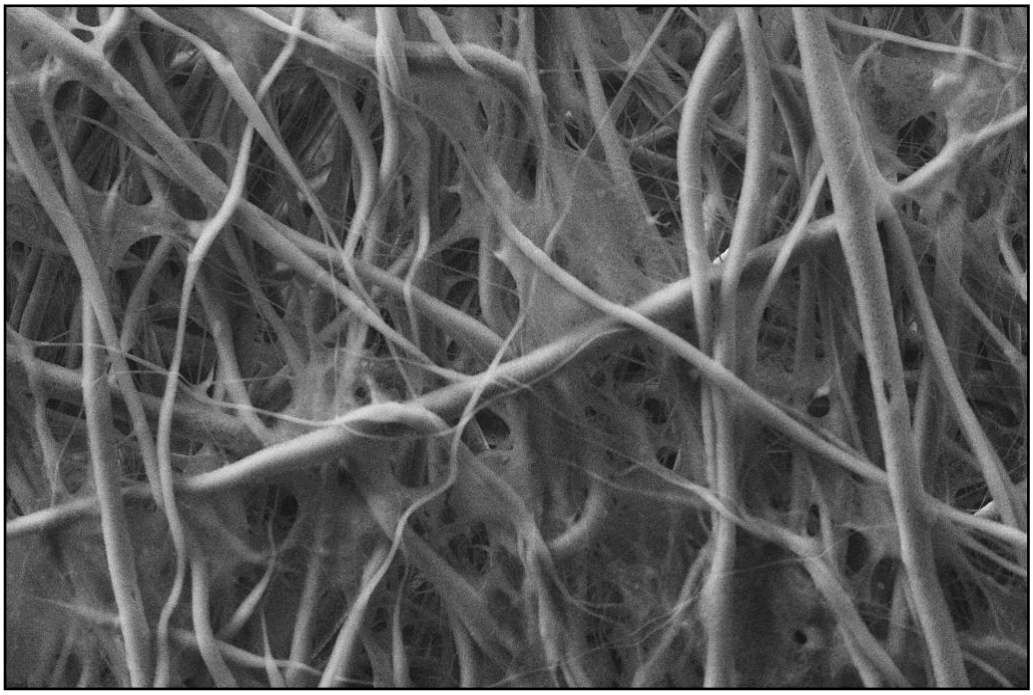

Figure 3.9. Morphology of the HASCs on PCL on the 3rd day of proliferation.

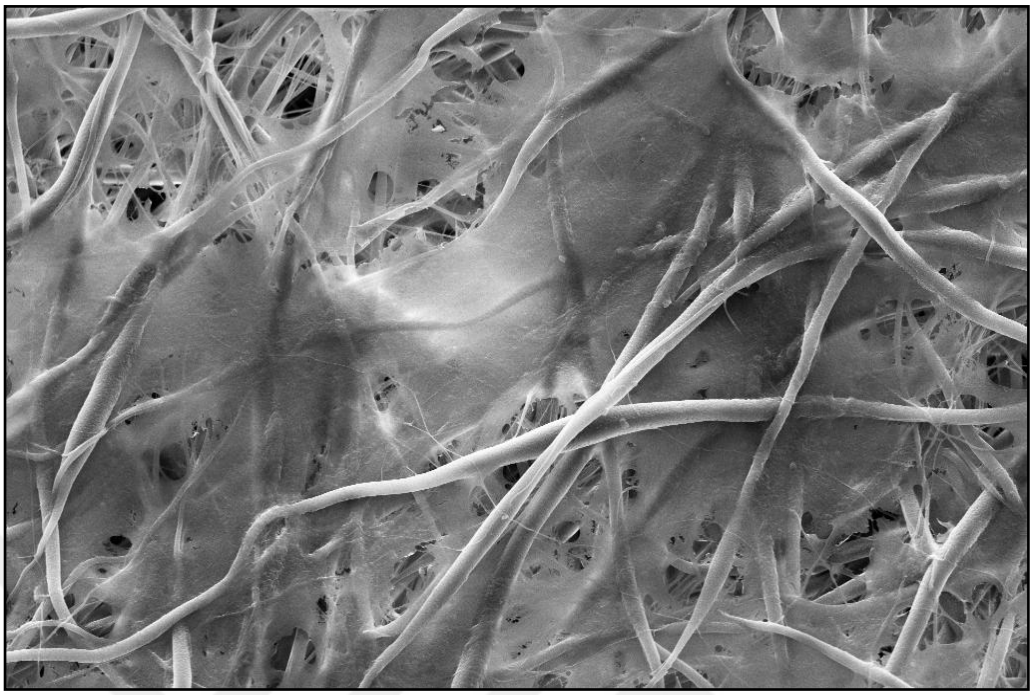

Figure 3.10. Morphology of the HASCs on PCL/AuNPs on the 3rd day of proliferation.

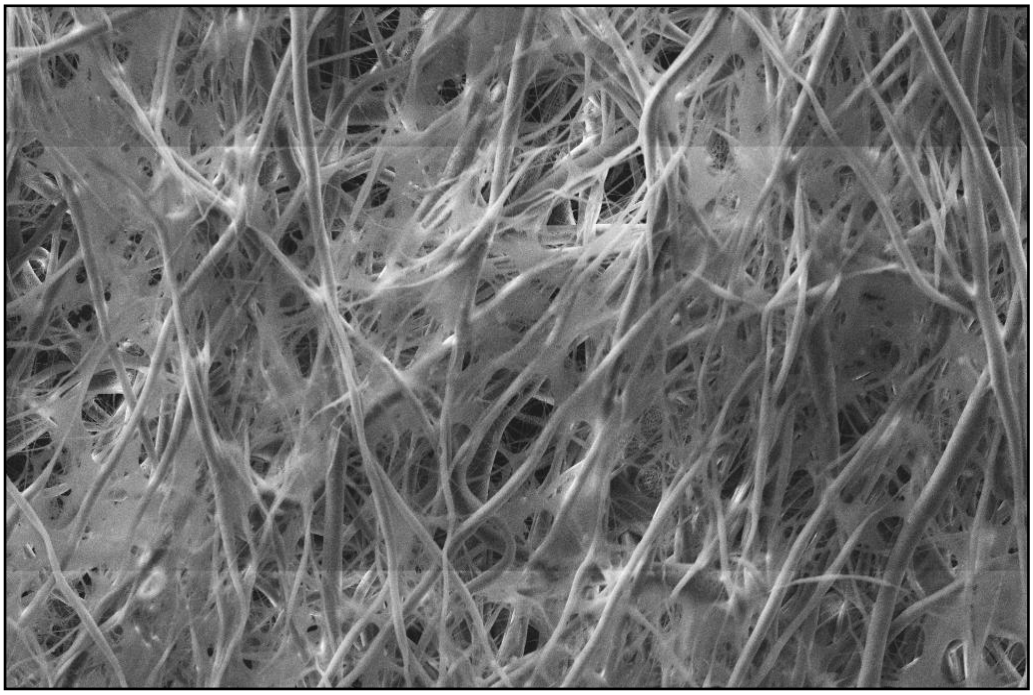

Figure 3.11. Morphology of the HASCs on PCL on the 7th day of proliferation.

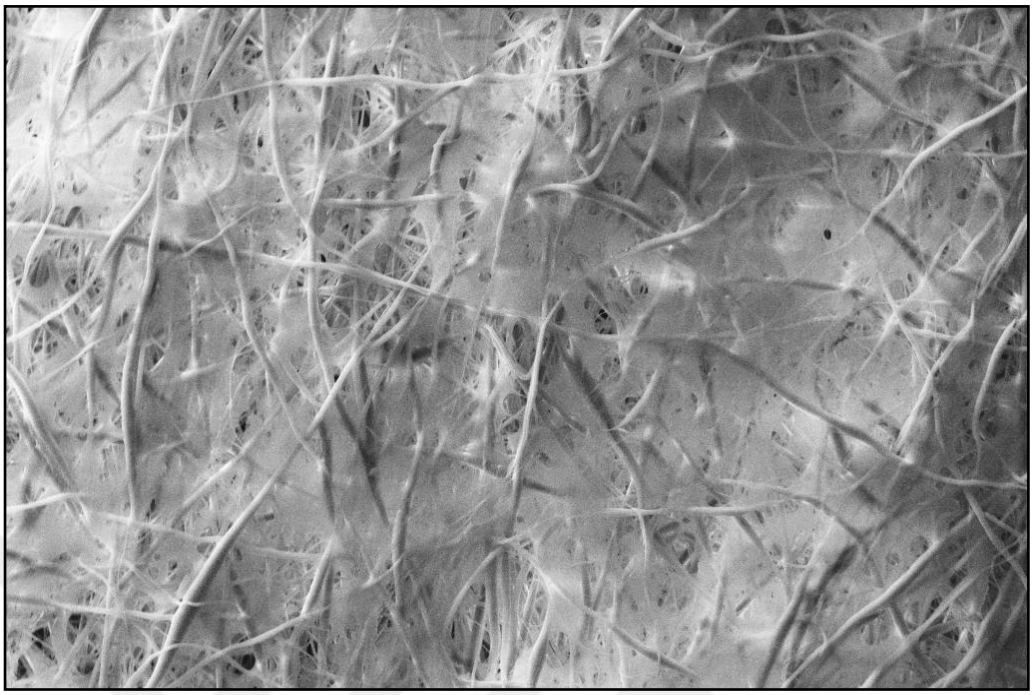

Figure 3.12. Morphology of the HASCs on PCL/AuNPs on the 7th day of proliferation.

3.3. VIABILITY OF HASC CELLS

WST-1 assay was performed to assess the viabilty of HASCs on PCL and PCL/AuNPs micro-fibrous scaffolds after 7 days of incubation. As shown Figure 3.13., the viability of HASCs adhered on PCL and PCL/AuNPs scaffolds was similar indicating that the incorporation of AuNPs into PCL scaffolds might not have an adverse effect on the proliferation and differentiation.

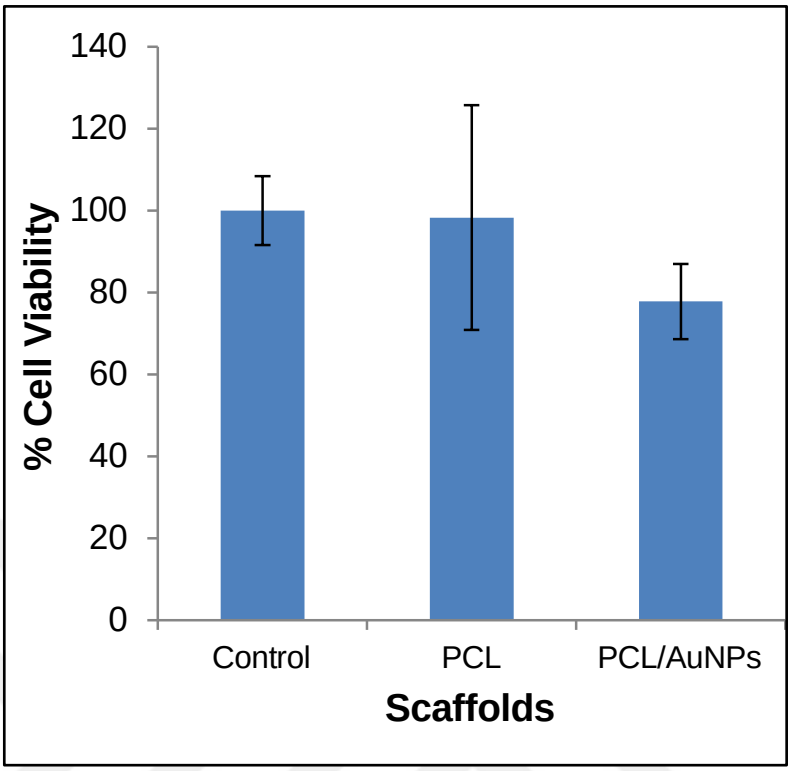

Figure 3.13. WST-1 results of HASCs on PCL and PCL/AuNPs micro-fibrous scaffolds after 7 days of cell seeding.

3.4. ELECTRICAL STIMULATION

PCL scaffolds prepared by electrospinning technique and also, AuNPs were incorporated into PCL scaffolds for the electrical conduction. The HASCs seeded on PCL and PCL/AuNPs micro-fibrous scaffolds. The external electrical stimulation was applied 100 mV and 10 min a day because 100 mV was measured to be the optimal electrical field by Basu and his colleague [38].

3.5. FLOW CYTOMETRY ANALYSIS

The differentiation of HASCs to neuronal cells on PCL and PCL/AuNPs micro-fibrous scaffolds was determined by flow cytometry analysis as shown in Figure 3.14. The differentiation of HASCs into neuronal cells on PCL and PCL/AuNPs micro-fibrous scaffolds were found to express the neuronal proteins such as β-III-tubulin and MAP-2

(microtubule associated protein) after 5 days of 100 mV 10 min/day electrical stimulation. Figure 3.14. shows β-III-tubulin, which is a microtubule element protein, was expressed from differentiated HASCs. Also, low level of MAP-2 expression was observed from differentiated HASCs.

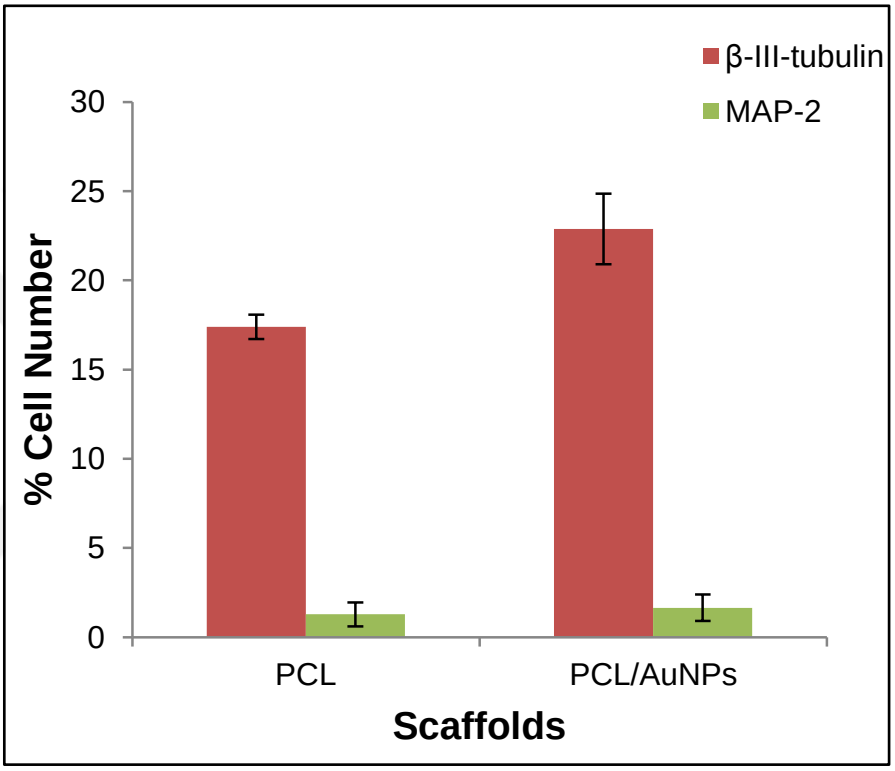

Figure 3.14. Flow cytometry analysis of the differentiated HASCs. The expression of β-III-tubulin protein from differentiated HASCs on PCL scaffolds and PCL/AuNPs (red). The expression of MAP-2 protein from differentiated HASCs on PCL scaffolds and PCL/AuNPs (green).

3.6. PHENOTYPIC CHARACTERIZATION BY IMMUNOSTAINING

The adhered HASCs on PCL and PCL/AuNPs micro-fibrous scaffolds were examined for morphological changes after 5 days of electrical stimulation of 100 mV for 10 min. Figure 3.15. shows general images of nestin stained HASCs on PCL scaffold (a) and AuNPs/PCL scaffold (b). As seen the number of cell differenitiated is increased on AuNPs/PCL scaffold compared to the PCL scaffold. The HASCs cultured on PCL and PCL/AuNPs

micro-fibrous scaffolds showed well adhered morphology, which supported the cell growth and proliferation.

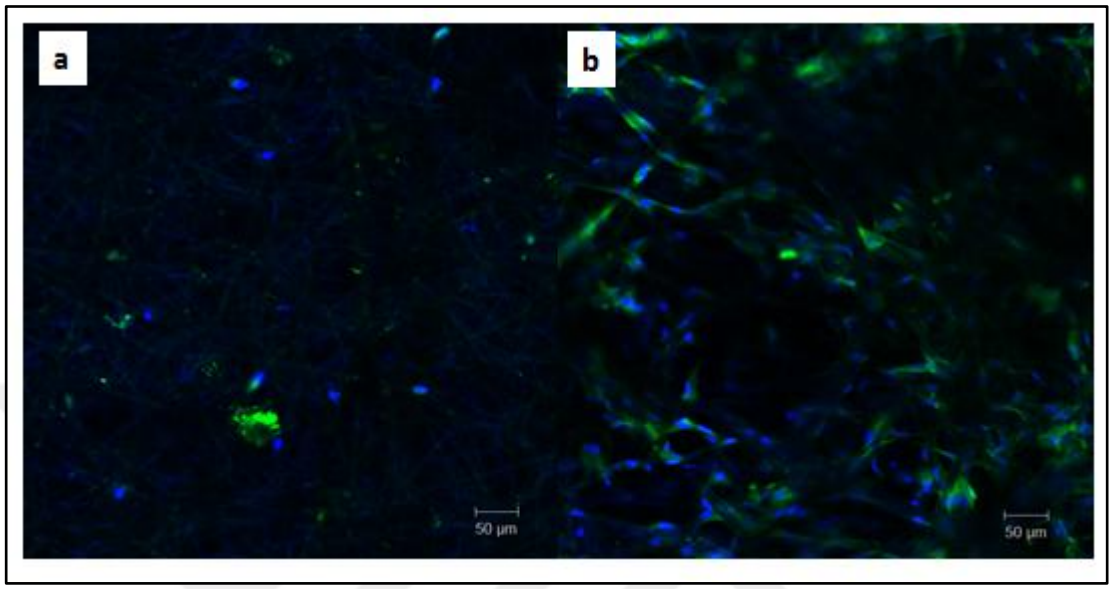

Figure 3.15. A general view of confocal images of immunocytochemically stained cells on PCL scaffold (a) and AuNPs/PCL scaffold (b). Labeled antibodies target intermediate filament proteins expressed in nerve cells. (A 10x objective was used for imaging)

The HASCs were immunostained with nestin, which is a known neurogenic differentiation marker after 5 days of electrical stimulation on PCL scaffold as seen from different regions in Figure 3.16.

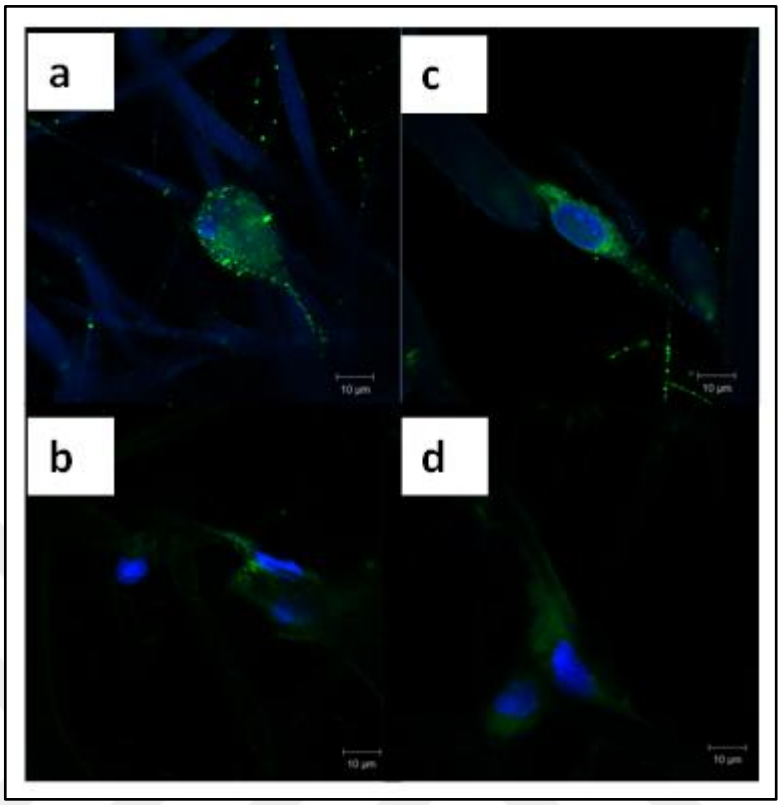

Figure.3.16.Immunocytochemical staining showing the expression of nestin marker for neuronal cells on PCL scaffold from different regions(a,b,c,d) after 5 days of electric field stimulation with 100 mV/cm in cycle of 10 min/day. Nestin marker was showed green and the nuclei were stained with Hoechst 33258 (blue).

Figure 3.17. shows the confocal images of HASCs on AuNPs/PCL scaffold from different regions (Figure 3.17. a,b,c,d). As seen, nestin was highly expressed in HASCs on AuNPs/PCL scaffold after electrical stimulation.

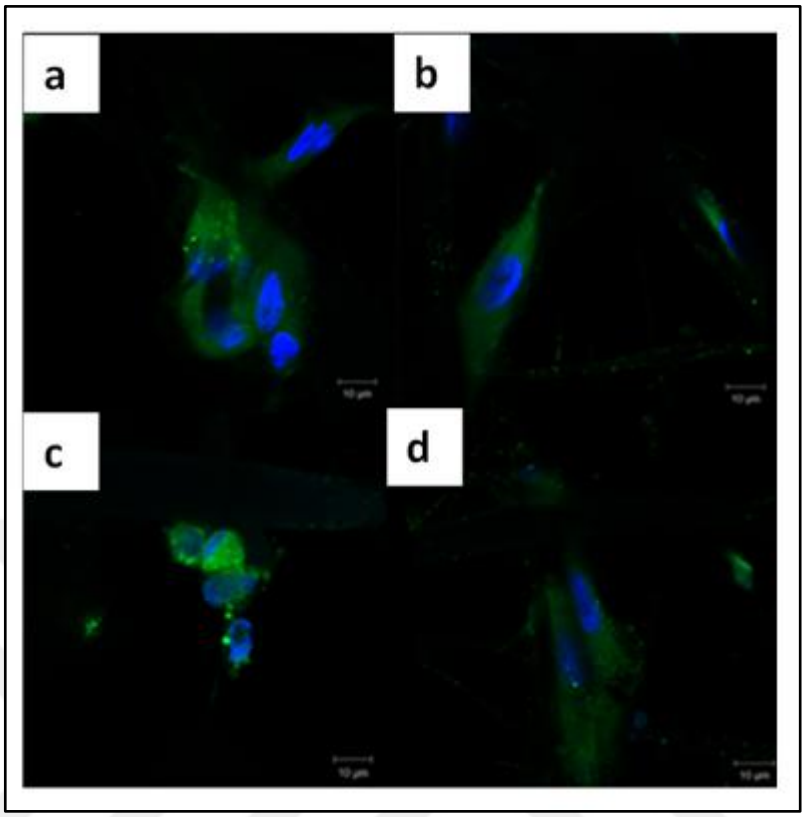

Figure 3.17. Immunocytochemical staining showing the expression of nestin marker for neuronal cells on PCL/AuNPs scaffold from different regions(a,b,c,d) after 5 days of electric field stimulation with 100 mV/cm in cycle of 10 min/day. Nestin marker was showed green and the nuclei were stained with Hoechst 33258 (blue).

Figure 3.18. shows general images of β-III-tubulin immuno stained differentiated HASCs on PCL scaffold (a) and AuNPs/PCL scaffold (b). As seen in Figure 3.18. the number of HASCs differenitiated is increased on AuNPs/PCL scaffold compared to the PCL scaffold. The HASCs cultured on PCL and PCL/AuNPs micro-fibrous scaffolds showed well adhered morphology, which supported the cell growth and proliferation.

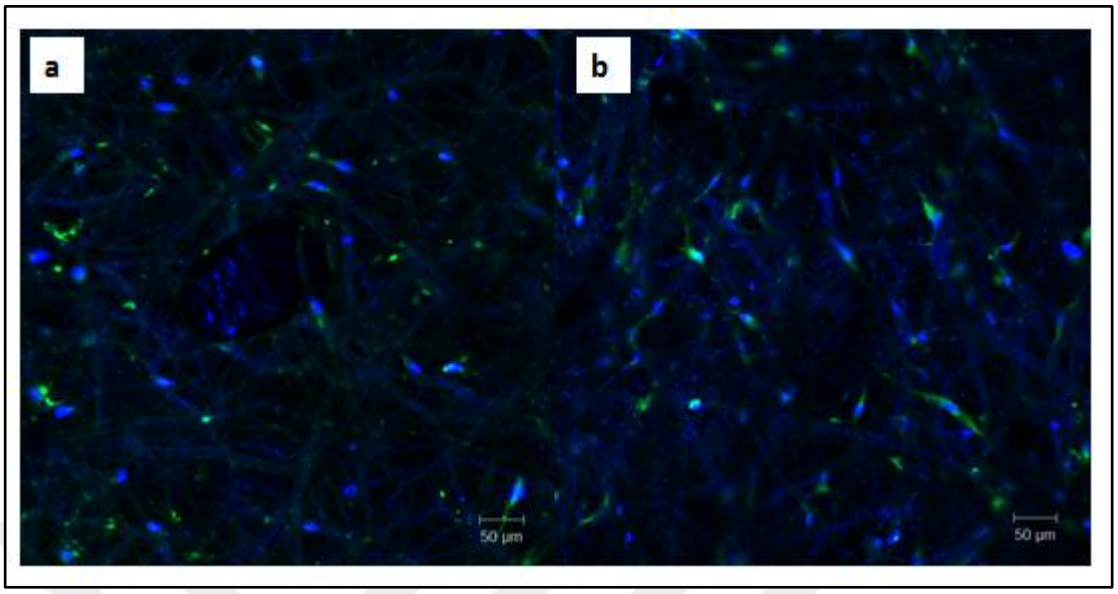

Figure 3.18. A general view of confocal images of immunocytochemically stained cells on PCL scaffold (a) and AuNPs/PCL scaffold (b). Labeled antibodies target microtubule element proteins expressed in nerve cells. (A 10x objective was used for imaging)

β-III-tubulin expression was determined after 5 days of electrical stimulation of 100 mV for 10 min a day as seen from different region on PCL scaffold in Figure 3.19. (a, b, c, d).

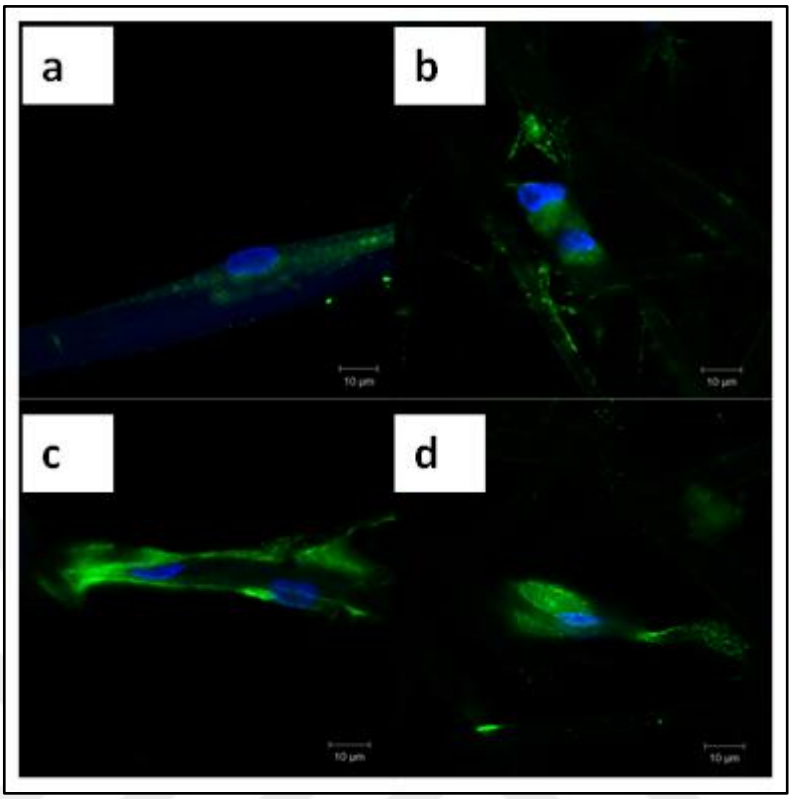

Figure 3.19. Immunocytochemical staining showing the expression of β-III-tubulin marker for neuronal cells on PCL scaffold from different regions(a,b,c,d) after 5 days of electric field stimulation with 100 mV/cm in cycle of 10 min/day. β-III-tubulin marker was showed green and the nuclei were stained with Hoechst 33258 (blue).

Figure 3.20. shows the confocal images of adhered HASCs on AuNPs/PCL scaffold from different regions (Figure 3.20. a,b,c,d). As seen, β-III-tubulin was highly expressed in HASCs on AuNPs/PCL scaffold after 5 days of electrical stimulation.

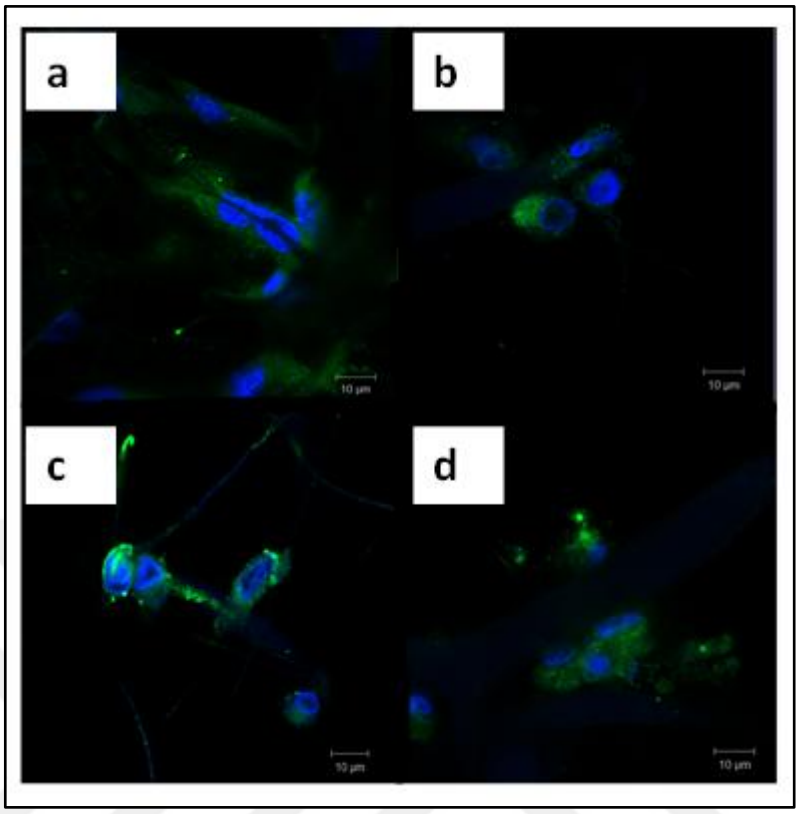

Figure 3.20. Immunocytochemical staining showing the expression of β-III-tubulin marker for neuronal cells on AuNPs/PCL scaffold from different regions(a,b,c,d) after 5 days of electric field stimulation with 100 mV/cm in cycle of 10 min/day. β-III-tubulin marker was showed green and the nuclei were stained with Hoechst 33258 (blue).

4. DISCUSSION

The poly (ε -caprolactone) (PCL) has been commonly used as a biocompatible and biodegradable polymer in tissue engineering. It has many properties such as suitability for the fabrication of the nerve regeneration, low degree of swelling behavior and degrading capacity. On the other hand, PCL has both weak hydrophilic property and lack of functional groups, which cause low cell adhesion and cell proliferation on PCL scaffolds. In recent years, a few techniques have been developed to overcome cell adhesion and proliferation problems of PCL scaffolds. The techniques include nanoparticle assembly on the surface, layer-by-layer multilayer assembly of polymer and simple physical adsorption. Incorporation of nanoparticle into the polymer matrix or assembly on surface allows variety of applications of such materials in including catalysis, sensing devices and tissue engineering scaffolds.

In this study, gold nanoparticles (AuNPs) were incorporated into non-conductive polymer PCL. Furthermore, 5 nm to 7 nm AuNPs do not have toxic effect for cells. The AuNPs also give partial novel properties such as electrical conduction and stimulate cell growth directly when they are incorporated into PCL. To the best of my knowledge, there are no reports utilizing PCL/AuNPs micro-fibrous scaffolds for tissue engineering in literature. The AuNPs reduced by aqueous alkaline sodium borohydride ($NaBH_4$) are blended into the PCL polymer to provide conductivity to the scaffold. The blended technique was found to be a very efficient technique to modify PCL micro-fibrous scaffolds for tissue engineering. In this study, the preparation and characterization of tissue scaffolds from PCL by incorporating into AuNPs were demonstrated. In this respect, PCL/AuNPs scaffolds were used to stimulate Human adipose stem cells (HASCs) to differentiate to neural cells through electrical current.

The contact angle measurement results demonstrated that AuNPs modification of PCL scaffolds improved surface wettability of the scaffolds and changed the micro-fibrous size (Table 3.1. and Figures 3.1.,3.4.,3.5.,3.6.). This result exhibited that the increase in the surface wettability of the PCL/AuNPs scaffolds leads to improved cell attachment, spreading and proliferation. Furthermore, UV- visible spectroscopy was obtained for 4.8 nm and 5.6 nm AuNPs as seen Figure 3.2. proves that synthesized AuNPs in water and toluene have different sizes makes conclusions of different spectrums. Figure 3.3. shows

the AFM images of the synthesized AuNPs. Although DLS data shows that the average size of AuNPs is 5.6 ± 2 nm, AFM analysis indicates larger size of AuNPs. This could be possibly be due to the aggregation of the particles as the droplet of colloidal suspension is spotted to dry.Taken together, this micro-fibrous PCL/AuNPs scaffold structure will be of biological interest because these microstructures present topography that has structural similarity to natural ECM.

Cell adhesion is the most important response when cells contact with scaffold material. Consequently, HASCs were cultured on the micro-fibrous PCL and PCL/AuNPs scaffolds and their cell adhesion relative to the control scaffolds after 1, 3 and 7 days of incubation was observed with SEM as shown Figures 3.7. to 3.12. Micro-fibrous scaffold with AuNPs was favored for initial adhesion of HASCs. This observation can be explained by the hydrophilicity provided by AuNPs and more attachment sites for the cells to contact and adhere. This observation also suggests that the as-grown micro-fibrous scaffolds were chemically stable since they were not degraded by the culture medium. Moreover, the stability and strength examination of these as-grown PCL/AuNPs micro-fibrous scaffolds *in vivo* would be valuable.

The viability of the HASCs on PCL and PCL/AuNPs micro-fibrous scaffolds was evaluated using WST-1 assay, which depends on the cleavage of the WST-1 tetrazolium salt to the colorimetric formazan by the mitochondrial activity in viable cells. In Figure 3.13., the adhered HASCs cultured for 7 days of viability on PCL and PCL/AuNPs micro-fibrous scaffolds are shown. Cell viability was observed same in both PCL and PCL/AuNPs micro-fibrous scaffolds.

The differentiation of HASCs into neuronal cells on PCL and PCL/AuNPs micro-fibrous scaffolds was observed by analysing β-III-tubulin and MAP-2 on flow cytometry. β-III-tubulin exists specifically in neurons. β-III-tubulin is a well-defined marker of neuronal cells. MAP-2, which is found in dendrites, provide microtubule stabilizing in the cells. β-III-tubulin expression from the differentiated HASCs on PCL/AuNPs micro-fibrous scaffold is much more than the differentiated HASCs on PCL scaffold. However, MAP-2 expression was not significantly different between differentiated HASCs on PCL and PCL/AuNPs scaffolds, as seen in Figure 3.14. Taken together, the PCL/AuNPs scaffolds conduct electricity and contribute differentiation of HASCs.

The differentiation of HASCs to neuronal cells on PCL and PCL/AuNPs micro-fibrous scaffolds was assessed by immunocytochemistry of nestin and β-III-tubulin. The adhered HASCs stimulated with 100 mV electric 10 min/day for differentiation to neuronal cells. Nestin expression, which is a neuronal precursor molecule, indicates potential neurogenic capacity. Also, β-III-tubulin protein is a microtubule element of brain and is just found neurons. Nestin and β-III-tubulin markers, which are expressed in mature neurons, were used for the detection of neurogenic markers. Nestin and β-III-tubulin protein staining showed that HASCs differentiated into neuronal cells by electrical stimulation (Figure 3.15, 3.16, 3.17, 3.18, 3.19, 3.20.).

In summary, the results show that the electrical stimulation affects HASCs to differentiate without any neuronal growth factor. The HASCs cultured on PCL and PCL/AuNPs micro-fibrous scaffolds and stimulated with electrical field 100 mV for 5 days 10 min/day. The results indicate electrical conduction may give to change in the morphology and gene expression profile that may resemble neuronal cells. Thus, PCL/AuNPs micro-fibrous scaffold can be an excellent ECM for HASCs for the adhesion and proliferation and external electric stimuli effective physical cue for manipulating the cell functionality *in vitro.*

5. CONCLUSION

In this thesis, it is demonstrated that AuNPs incorporated into PCL microfiber scaffolds and thier electrical stimulation affect the HASCs differentiation. The electrical stimulation of PCL/AuNPs microfibers did not only enhance the differentiation into neural lineages but also helped with neurite outgrowth. This study suggests the further investigation of in depth, which may enhance tissue engineering with stem cells therapy for nerve repair.

REFERENCES

1. R. Langer and P. J. Vacanti. Tissue Engineering. *Science* 260: 920-926, 1993

2. T.A. James. Embryonic stem cell lines derived from human blastocysts. *Science* 282: 1145-1147, 1998.

3. A. Schäffler, and C. Büchler. Concise review: adipose tissue-derived stromal cells basic and clinical implications for novel cell-based therapies. *Stem Cells* 25: 818-827, 2007.

4. P. Bourin, B.A. Bunnell, L. Casteilla, M. Dominici, A.J. Katz, K.L. March, H. Redl, J.P. Rubin, K. Yoshimura and J.M. Gimble. Stromal cells from the adipose tissue-derived stromal vascular fraction and culture expanded adipose tissue-derived stromal/stem cells: a joint statement of the International Federation for Adipose Therapeutics and Science (IFATS) and the International Society for Cellular Therapy (ISCT). *Cytotherapy* 15: 641-648, 2013.

5. M. Hiroshi, M. Tobita, and A.C. Uysal. Concise review: adipose-derived stem cells as a novel tool for future regenerative medicine. *Stem Cells* 30: 804-810, 2012.

6. C.I. Arnold Adult mesenchymal stem cells for tissue engineering versus regenerative medicine. *Journal of Cellular Physiology* 213: 341-347, 2007.

7. P.B Malafaya, G.A. Silva, and R.L. Reis. Natural–origin polymers as carriers and scaffolds for biomolecules and cell delivery in tissue engineering applications. *Advanced Drug Delivery Reviews* 59 :207-233, 2007.

8. S. Anuradha, U.M. Krishnan and S. Sethuraman. Development of biomaterial scaffold for nerve tissue engineering: Biomaterial mediated neural regeneration. *Journal of Biomedical Science* 16: 108, 2009.

9. F. Berthiaume, P.V. Moghe, M. Toner and M.L. Yarmush. Effect of extracellular matrix topology on cell structure, function, and physiological responsiveness: hepatocytes cultured in a sandwich configuration. *The FASEB Journal* 10: 1471-1484, 1996.

10. W.J. Li, R.L. Mauck, and R.S. Tuan. Electrospun nanofibrous scaffolds: production, characterization, and applications for tissue engineering and drug delivery. *Journal of Biomedical Nanotechnology* 1: 259-275, 2005.

11. X. Liu and P.X. Ma. Phase separation, pore structure, and properties of nanofibrous gelatin scaffolds. *Biomaterials* 30: 4094-4103, 2009.

12. F. Yang, Fabrication of nano-structured porous PLLA scaffold intended for nerve tissue engineering. *Biomaterials* 25: 1891-1900, 2004.

13. R.A. Jain. The manufacturing techniques of various drug loaded biodegradable poly (lactide-co-glycolide)(PLGA) devices. *Biomaterials* 21: 2475-2490, 2000.

14. J. Zhao. Preparation, structure and crystallinity of chitosan nano-fibers by a solid–liquid phase separation technique. *Carbohydrate Polymers* 83: 1541-1546, 2011.

15. J.D. Hartgerink, E. Beniash and S.I. Stupp. Self-assembly and mineralization of peptide-amphiphile nanofibers. *Science* 294: 1684-1688, 2001.

16. R. Fairman and K.S. Åkerfeldt. Peptides as novel smart materials. *Current Opinion in Structural Biology* 15: 453-463, 2005.

17. L.A. Smith and P.X. Ma. Nano-fibrous scaffolds for tissue engineering. *Colloids and Surfaces b: Biointerfaces* 39: 125-131, 2004.

18. C.P. Barnes, Nanofiber technology: designing the next generation of tissue engineering scaffolds. *Advanced Drug Delivery Reviews* 59: 1413-1433, 2007.

19. M. Goldberg, R. Langer and X. Jia. Nanostructured materials for applications in drug delivery and tissue engineering. *Journal of Biomaterials Science, Polymer Edition* 18: 241-268, 2007

20. Q.P. Pham, U. Sharma, and A.G. Mikos. Electrospinning of polymeric nanofibers for tissue engineering applications: a review. *Tissue Engineering* 12: 1197-1211, 2006.

21. Z. Huang, Y. Zhang, S. Ramakrishna and C. Lim. Electrospinning and mechanical characterization of gelatin nanofibers. *Polyme*r 45: 5361, 2004.

22. S.I. Jeong, M.D. Krebs, C.A. Bonino, J.E. Samorezov, S.A. Khan and E. Alsberg. Electrospun chitosan-alginate nanofibers with in situ polyelectrolyte complexation for use as tissue engineering scaffolds. *Tissue Engineering Part A* 17: 59, 2011.

23. Y. Young. In vitro degradation behavior of electrospun polyglycolide, polylactide, and poly (lactide-co-glycolide). *Journal of Applied Polymer Science* 95: 193-200, 2005.

24. W.J. Li. Multilineage differentiation of human mesenchymal stem cells in a three-dimensional nanofibrous scaffold. *Biomaterials* 26: 5158-5166, 2005.

25. M. Hronik-Tupaj. Osteoblastic differentiation and stress response of human mesenchymal stem cells exposed to alternating current electric fields. *Biomedical Engineering Online* 10: 9, 2011.

26. S. Sun, I. Titushkin and C. Michael. Regulation of mesenchymal stem cell adhesion and orientation in 3D collagen scaffold by electrical stimulus. *Bioelectrochemistry* 69: 133-141, 2006.

27. H. Zhao, H. Xie, H. Liu, H. Chen, Y. Jiao and W. Wu. Implanted spike wave electric stimulation promotes survival of the bone marrow mesenchymal stem cells and functional recovery in the spinal cord injured rats. *Neuroscience Letters* 491: 73-78, 2011.

28. S. McLaughlin, and M.M. Poo. The role of electro-osmosis in the electric-field-induced movement of charged macromolecules on the surfaces of cells. *Biophysical Journal* 34: 85, 1981.

29. M.R. Cho, H.S. Thatte, M.T. Silvia and D.E. Golan. Transmembrane calcium influx induced by ac electric fields. *The FASEB Journal* 13: 677-683, 1999.

30. A. Rajnicek, S. Britland and C. McCaig. Contact guidance of CNS neurites on grooved quartz: influence of groove dimensions, neuronal age and cell type. *Journal of Cell Science* 110: 2905-2913, 1997.

31. M. Zhao, A. Dick, J.V. Forrester and C.D. McCaig. Electric field–directed cell motility involves up-regulated expression and asymmetric redistribution of the epidermal growth factor receptors and is enhanced by fibronectin and laminin. *Molecular Biology of The Cell* 10: 1259-1276, 1999.

32. M. Yamada, K. Tanemura, K. Okada, S. Iwanami, A. Nakamura, M. Mizuno and H.T. Kondo. Electrical stimulation modulates fate determination of differentiating embryonic stem cells. *Stem Cells* 25: 562-570, 2007.

33. M.E. Mycielska and M.B.A. Djamgoz. Cellular mechanisms of direct-current electric field effects: galvanotaxis and metastatic disease. *Journal of Cell Science* 117: 1631-1639, 2004.

34. M.O. Alvarez, P.M. Mertz, R.V. Smerbeck and W.H. Eaglstein. The healing of superficial skin wounds is stimulated by external electrical current. *Journal of Investigative Dermatology* 81: 144-148, 1983.

35. S.E. Gardner, A.R. Frantz and F.L. Schmidt. Effect of electrical stimulation on chronic wound healing: a meta-analysis. *Wound Repair and Regeneration* 7: 495-503, 1999.

36. D. Perry. Treatment of symptomatic abnormal skin scars with electrical stimulation. *Journal of Wound Care* 19: 447, 2010.

37. N.M. Martin, J.I. Basham, P. Chando and S.K. Eah. Charged gold nanoparticles in non-polar solvents: 10-min synthesis and 2D self-assembly. *Langmuir* 26: 7410-7417, 2010.

38. A.K. Dubey and B. Basu. Pulsed Electrical Stimulation and Surface Charge Induced Cell Growth on Multistage Spark Plasma Sintered Hydroxyapatite-Barium Titanate Piezobiocomposite. *Journal of the American Ceramic Society* 97: 481-489, 2014.

39. The Iran Project, "Iranian Researchers Build Nanofibers for Severe Burns Recovery" http://theiranproject.com/blog/2013/08/19/iranian-researchers-build-nanofibers-for-severe-burns-recovery/ [retrieved 27 August 2015].